Suppression of the Wing-Body Junction Vortex by Body Surface Suction

D. B. Philips,* J. M. Cimbala,† and A. L. Treaster‡
Pennsylvania State University, University Park, Pennsylvania 16802

A horseshoe-shaped vortex, known as a wing-body junction vortex or horseshoe vortex, forms when spanwise vorticity in the boundary layer along a surface wraps around a wing protruding from the surface. In the past, various techniques of suppressing the wing-body junction vortex have been attempted. Reported here is a novel approach whereby the oncoming wall boundary layer is removed by suction along the body surface immediately upstream of the wing. The idea is that elimination of the boundary layer essentially removes the spanwise vorticity, and inhibits the formation of a wing-body junction vortex. To test this concept experimentally, velocity data were acquired via five-hole probe surveys in a plane normal to one of the walls of a semi-infinite symmetrical airfoil. Differentiation of these data yielded mean streamwise vorticity contours and values of net circulation. In the unmodified (no suction) case, the streamwise leg of the horseshoe vortex was clearly identified. The addition of suction successfully reduced the size and circulation of the large scale vortex. In fact, at a suction volumetric flow rate of about twice that through the boundary layer, the large scale horseshoe vortex could no longer be found for our configuration.

Nomenclature

Q_{bl}	=	boundary-layer volumetric flow rate
Q_s	=	suction volumetric flow rate
Q^*	=	nondimensional suction volumetric flow rate $= Q_s/Q_{bl}$
T	=	maximum wing thickness (140 mm)
U_∞	=	freestream velocity (X direction)
X, Y, Z	=	Cartesian coordinate system (See Fig. 1)
Γ	=	circulation
Γ^*	=	nondimensional circulation $= \Gamma/(TU_\infty)$
Δ	=	grid spacing in measurement plane
δ	=	99% boundary-layer thickness
δ^*	=	boundary-layer displacement thickness
θ	=	boundary-layer momentum thickness
$\omega_x, \omega_y, \omega_z$	=	Cartesian vorticity components

Introduction

THE flowfield at a wing-body junction is complicated because of the three-dimensional interaction between the approaching body boundary layer and the pressure field produced by the wing. Because of the adverse pressure gradient imposed on the body boundary layer, the flow separates ahead of the junction, and a vortex is formed from the spanwise vorticity (ω_z) in the boundary layer. This vortex is stretched and intensified as it is forced to wrap around the wing. This phenomenon is also referred to as a "horseshoe vortex," because of its shape (see Fig. 1). The coordinate system used in this study is also shown in Fig. 1.

The effects of the horseshoe vortex on the flowfield and downstream mechanical devices are usually undesirable. The vortex structure is well-known to be unsteady, and thus can create unwanted vibration and dynamic stresses. Furthermore, the swirling action of the vortex acts to pump high-momentum fluid from the freestream into the near body region. This can adversely affect the wing lift characteristics, as well as increase surface shear stresses and thus drag. This pumping action can also increase local heat transfer properties at the surfaces, which at times may be of concern.

Previous Studies

There have been many attempts to reduce the strength of the horseshoe vortex by modifying the geometry of a standard blunt nosed airfoil. In the 1984 paper of Mehta,[1] he reports the findings of an experimental study comparing the effect of various two-dimensional wing leading-edge shapes on the vortex size and strength. As predicted by theory, a somewhat weaker and smaller vortex is created when a less blunt leading-edge geometry is used.

Kubendran et al.[2] performed experiments with leading-edge swept fairings, while Sung and Lin[3] studied the use of both leading- and trailing-edge swept fairings. In both of these studies, the vortex strength was reduced. Devenport et al.[4] showed that complete fillets in the wing-body corner effectively created a larger nose radius and thus a blunter wing leading edge. Therefore the vortex seemed actually stronger and larger with the fillet than without. Recent experiments of Maughmer et al.[5] showed that drag can be reduced by careful design of the wing-body junction region.

The above geometry modifications aimed at reducing the horseshoe vortex strength were somewhat successful, but none could eliminate the phenomenon totally, since spanwise vorticity in the wall boundary layer was not removed. Barber[6] varied the distance from the wing-body junction to the body leading edge, effectively controlling the approaching body boundary-layer thickness. It was found that the smaller the boundary layer, the smaller was the region of influence of the vortex; but no quantitative data were presented from which the vortex strength could be estimated. Barber's work also showed that due to the lack of the large vortex, and thus its inherent mixing action, separation off the wing trailing edge occurred prematurely.

There has also been at least one attempt to directly remove the horseshoe vortex downstream of the wing-body junction region. Vortex generators were applied by McGinley[7] to cancel the vorticity in the streamwise vortex legs. This system worked well, but the correct location, size, and orientation

Received Nov. 3, 1990; revision received Feb. 17, 1991; accepted for publication March 5, 1991. Copyright © 1991 by the American Institute of Aeronautics and Astronautics, Inc. All rights reserved.

*Graduate Research Assistant, Department of Mechanical Engineering; currently, Researcher, Battelle Columbus Laboratories, Columbus, OH 43201.

†Associate Professor, Department of Mechanical Engineering. Member AIAA.

‡Research Associate, Applied Research Laboratory Penn State. Member AIAA.

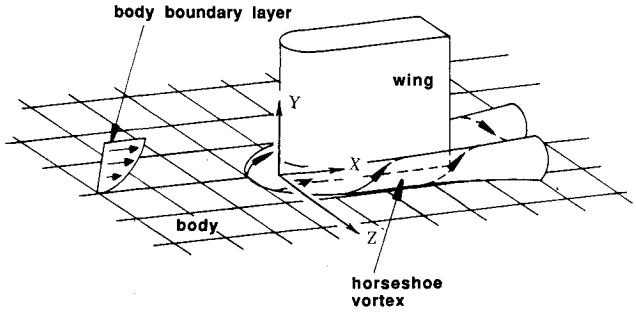

Fig. 1 Schematic of the flowfield and coordinate system.

of the generators may be too sensitive to too many factors for this approach to work well in an operating system.

Current Objectives

It can be seen that many passive methods for manipulating the horseshoe vortex have been tried, and often with some success. But none have been totally successful in eliminating the undesired structure. The possibility of using suction at the body surface to reduce the vortex strength was investigated in this study. Suction at a wing-body junction was also investigated previously by Goldsmith,[8] but his efforts were concentrated on producing a laminar flowfield, and the horseshoe vortex problem was never specifically addressed. In the present study, two possible suction schemes were initially considered, i.e., suction of the approaching body boundary layer, and suction of the streamwise legs of the horseshoe vortex from the flowfield downstream of the junction. Only the former approach was explored. The idea is that elimination of the body boundary layer eliminates the spanwise vorticity from which the horseshoe vortex develops, and hence should inhibit its formation. This technique is therefore the only one that directly attacks the *source* of the horseshoe vortex, i.e., spanwise vorticity in the body boundary layer.

Experimental Apparatus and Procedure

Wind Tunnel and Instrumentation

This experimental research project was performed in the Subsonic Wind-Tunnel Facility of the Pennsylvania State University Mechanical Engineering Department. This open-loop, suction-type wind tunnel had an operating range of 0–15 m/s, a freestream turbulence intensity below 0.2%, and a test section 310 × 970 mm in cross section and 2.4 m in length.

An MKS Baratron differential pressure transducer in conjunction with an MKS high-accuracy signal conditioner supplied all pressure measurement needs for determining velocities in the wind tunnel. This system has a 1.0 mm Hg maximum range, with resolution down to 10^{-6} mm Hg. A Scanivalve system was employed to enable the monitoring of multiple pressures with this single transducer.

The high-pressure side of the transducer was connected to the stagnation pressure line of a pitot-static probe in the freestream. This acted as a universal reference pressure. The low-pressure side was connected to the output line of the Scanivalve, which could be switched to any of the holes of a five-hole probe. The five-hole probe was used in the nonnulling mode to make all of the three-dimensional velocity measurements. This angle-tube-type five-hole probe had a tip diameter of 1.7 mm and was hand made at the Pennsylvania State University's Applied Research Laboratory.

The five-hole probe was mounted on a two-dimensional traversing system, with computer-controlled stepper motors. The traversing system was installed to allow velocity measurements in a Y-Z plane. This system enabled positioning accuracy down to ± 6 μm.

Model Description

The wing-body junction was produced at the intersection of a wing model with the wind-tunnel wall. The model's leading edge was built around a 102-mm-diam aluminum duct. The body flaired out from this 102 mm thickness to a maximum constant thickness of $T = 140$ mm from the downstream half of the model. The total chord length was 900 mm, where the wing was chopped off sharply. The wing was 203 mm in span (Y direction), being supported on lag bolt legs. The model skeleton was wrapped with two layers of black poster board to provide sufficient rigidity. The goal was to create a model similar in shape to a symmetric airfoil with a semiinfinite chord. The final model presented a physical blockage of 9.3% of the test section cross-sectional area. The wing model was centered in the wind tunnel (Z direction), and its leading edge was 1.43 m downstream of the test section inlet. For all experiments, the boundary layer was tripped 610 mm upstream of the wing leading edge, the trip wire being 3.5 mm in diameter.

Suction System

Boundary-layer suction was applied through a 150-mm-wide (in the Z direction) by 190-mm-long (in the X direction) rectangular hole, located just upstream of the leading edge of the wing model, along the tunnel wall. The inside surface of this wall segment was covered with dense screening, to produce the required porous wall. Suction was applied at the hole by a variable-power centrifugal pump. By placing a pitot-static probe in the pump exit flow at various points, the suction volumetric flow rate Q_s was determined.

Experimental Procedure

The five-hole probe was calibrated at a velocity of 8.2 m/s. To minimize Reynolds-number effects on the five-hole probe, the wind tunnel speed was adjusted such that the probe took measurements near its calibration velocity. During measurements, a pitot-static probe was placed at approximately the same position as the five-hole probe, but on the opposite side of the model. This probe served two purposes; namely, it provided symmetry of the flowfield, and it monitored the streamwise velocity in the vortex leg. All experiments were performed at a freestream approach velocity of $U_\infty = 7.4$ m/s. Using the maximum wing thickness T as a length scale, this corresponds to a Reynolds number of 6.5×10^4. The five-hole probe was mounted on a Y-Z traversing system such that the probe tip was in a plane located at a streamwise position of $X = 215$ mm, where the wing thickness was 124 mm, i.e., still forward of the maximum thickness region. Grid points for data acquisition were evenly spaced at intervals of $\Delta = 2.0$ mm. The grid spanned an area from $Y = 2.0$ mm to $Y = 40.0$ mm, and from $Z = 70.0$ mm to $Z = 154.0$ mm ($0.50 < Z/T < 1.10$). The minimum Z position of 70.0 mm was 8 mm from the wing surface, at that streamwise location. These parameters specified a spatial grid of 860 points.

Once the velocity data were acquired, streamwise vorticity in the leg of the vortex could be determined by differentiation. However, since differentiation amplifies any randomness in the original data, the velocity data were first Fourier filtered by a two-dimensional Fourier algorithm, taken from the text by Press et al.[9] Cutoff wave numbers for the low-pass filter were 50 m^{-1} for the Y-frequency component, and 35 m^{-1} for the Z-frequency component. These cutoffs were used for all data sets. The filtered velocity data were then differentiated numerically to obtain streamwise vorticity data. Three different finite-difference techniques were used to calculate vorticity from the filtered velocity data—a diamond cell, a square cell, and a third-order scheme. The results were nearly indistinguishable for the three cases.

Utilizing the calculated vorticity values for this rectangular data grid with uniform spacing Δ, a net circulation was found using the following simplified equation:

$$\Gamma = \Delta^2 \sum_{ij} \omega_x \qquad (1)$$

The summation operation was performed over the spatial range from $Y = 7.0$ mm to $Y = 27.0$ mm, and from $Z = 80.0$ mm to $Z = 150.0$ mm. The net circulation provided a single value that summarized the measurements for an entire experiment. For further details on this procedure and the reported experimental results, see Philips.[10]

Experimental Results

For the first case, the suction system described previously was installed in the wind tunnel, but with no suction power applied. The pump exhaust was taped over to eliminate any chance of a net flow through the suction system. The 99% boundary-layer thickness δ was measured to be approximately 30 mm at the location of the leading edge of the wing model, but with the wing model removed. The boundary-layer displacement thickness was calculated to be $\delta^* \approx 9$ mm, and the momentum thickness was $\theta \approx 5$ mm.

The measured (unfiltered) mean velocity vectors in the Y-Z plane are shown in Fig. 2. This measurement plane slices through one leg of the horseshoe vortex at a streamwise position of $X = 215$ mm (X-$T = 1.54$ mm). The wing model surface was located at $Z = 62$ mm at this streamwise position. (The wind-tunnel wall coincides with the X-Z plane, as seen in Fig. 1.) The flow pattern in Fig. 2 seems odd at first glance. It is not at all obvious that a streamwise vortex is present. Keep in mind, however, that the streamwise location at which these data were measured corresponds to the forward portion of the wing, which is growing in thickness. Thus, the gross direction of the flow is to the right (away from the wing surface) in Fig. 2. There is also an upward flow (Y direction), probably due to the growing boundary layer on the body. Differentiation of these data to calculate streamwise vorticity effectively cancels out this gross flow direction. The computed streamwise vorticity contours corresponding to this velocity field are shown in Fig. 3. The contours are plotted in increments of 25 s^{-1}, with the thicker contour lines being multiples of 50 s^{-1}. Negative vorticity contours are shown as dashed lines, and the contour of 0 s^{-1} has not been plotted, for clarity. The observed flattened shape of the vortex agrees with the observations by Dickinson,[11] where he described it as a "tank track." The contour of maximum vorticity in Fig. 2 has a value of 100 s^{-1}, implying that the greatest calculated vorticity value was slightly in excess of 100 s^{-1}. In nondimensional form, $\omega_x T/U_\infty$ was somewhat greater than 1.9. There appears to be a double peak in the vorticity contour of Fig. 3. This is most likely due to lateral meandering of the vortex leg, which is quite unsteady. Similar bimodal results have been reported by Devenport and Simpson.[12] The net circulation for this case was calculated to be 0.086 m^2/s, or nondimensionally, $\Gamma^* = \Gamma/(TU_\infty) = 0.083$.

The porous section in the wind-tunnel wall through which the suction was applied was 150 mm wide (in the Z direction). The volumetric flow rate through a control volume enclosing the solid wall boundary layer, and being as wide as this porous section was calculated to be $Q_{bl} \approx 0.026$ m^3/s. If the suction

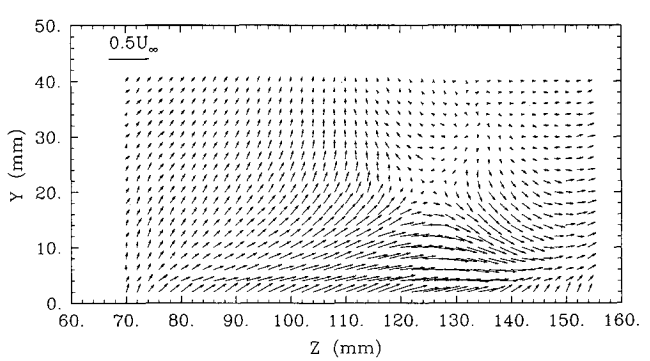

Fig. 2 Unfiltered velocity vectors in one leg of the horseshoe vortex for the case with no suction ($Q^* = 0.0$).

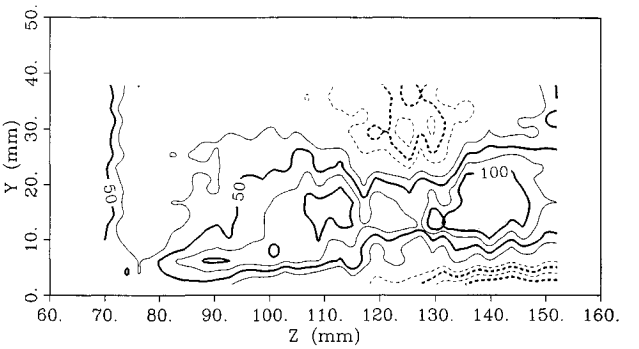

Fig. 3 Streamwise vorticity contours in one leg of the horseshoe vortex for the case with no suction ($Q^* = 0.0$).

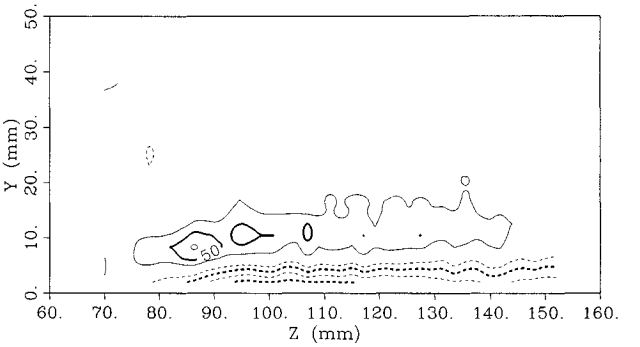

Fig. 4 Streamwise vorticity contours in one leg of the horseshoe vortex for the case with body suction applied ($Q^* = 1.2$).

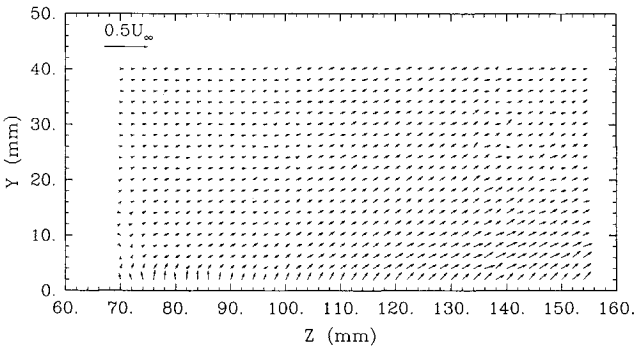

Fig. 5 Unfiltered velocity vectors in one leg of the horseshoe vortex for the case with body suction applied ($Q^* = 1.9$).

could be applied with 100% efficiency, Q_{bl} would be the minimum required flow rate to remove the entire boundary layer. Therefore this is a reference volumetric flow rate, to allow nondimensionalization of suction volumetric flow rates.

Suction experiments were performed at four different values of Q_s, the suction volumetric flow rate: 0.03 m^3/s, 0.04 m^3/s, 0.05 m^3/s, and 0.09 m^3/s. When divided by the boundary-layer volumetric flow rate, these correspond to nondimensional suction volumetric flow rates of $Q^* \approx 1.2$, 1.5, 1.9, and 3.5. The streamwise vorticity contour plot for the first of these is shown in Fig. 4. For small suction flow rates such as this, the horseshoe vortex was reduced in size and strength, but not completely suppressed. The net circulation for the case with $Q^* = 1.2$ was calculated to be 0.025 m^2/s ($\Gamma^* = 0.024$), a 71% decrease compared to that of the no-suction case.

The velocity vector and vorticity contour plots for the case with $Q^* = 1.9$ are shown in Figs. 5 and 6, respectively. At this suction rate, the leg of the large scale horseshoe vortex was no longer identifiable. The net circulation for this case decreased to about 0.014 m^2/s ($\Gamma^* = 0.013$).

With further increases in Q^*, the large scale vortex structure remains suppressed, but smaller spots of vorticity begin to

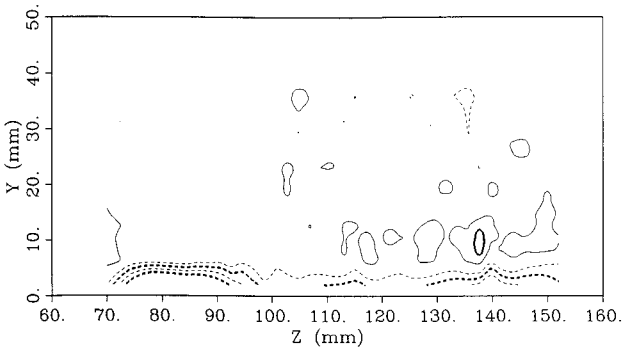

Fig. 6 Streamwise vorticity contours in one leg of the horseshoe vortex for the case with body suction applied ($Q^* = 1.9$).

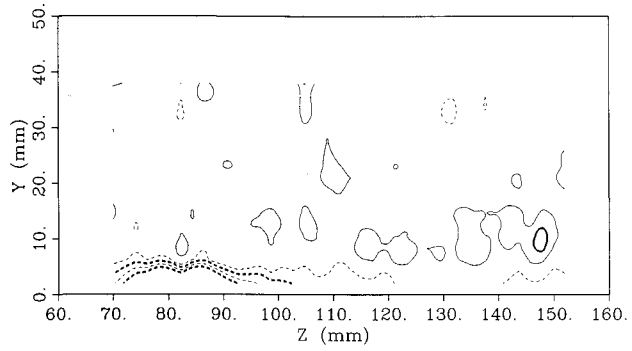

Fig. 7 Streamwise vorticity contours in one leg of the horseshoe vortex for the case with body suction applied ($Q^* = 3.5$).

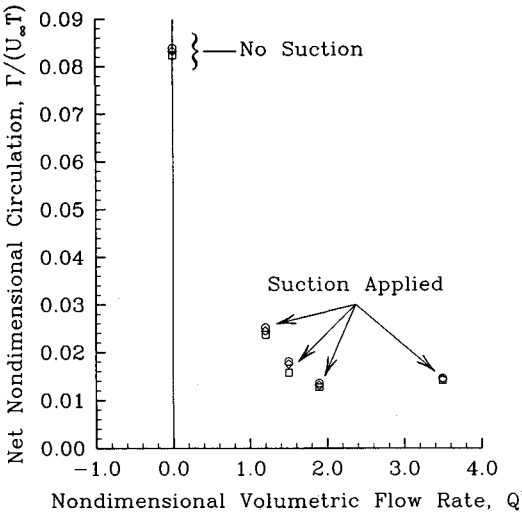

Fig. 8 Net nondimensional circulation in one leg of the horseshoe vortex as a function of nondimensional suction volumetric flow rate. Symbols represent the finite difference scheme used to calculate vorticity from the velocity field: ◇ = diamond cell, □ = square cell, ○ = third-order technique.

appear. For example, a spot of relatively high streamwise vorticity appears in the vicinity of $Y = 10$ mm and $Z = 145$ mm in Fig. 7 for the case with $Q^* = 3.5$. (A similar spot can also be seen in Fig. 6.) The position of this new structure implies that its origin was very likely the edge of the suction hole parallel to the X axis. This can be shown by adding half the wing thickness to half the suction hole width, yielding a sum of 145 mm. This vorticity production seems to have been due to the interaction between the normal flow (with a boundary layer—thus having a positive Y velocity) and the suction flow (boundary layer removed—thus having a negative Y velocity). This Y-velocity gradient is of the correct sign and location for generating the observed positive streamwise vorticity spot.

The calculated net nondimensional circulation for each of these suction experiments is summarized in Fig. 8 as a function of nondimensional suction volumetric flow rate. As mentioned previously, three different finite difference schemes were used to calculate the vorticity, but the results are nearly insensitive to the choice of scheme, as can be seen in Fig. 8.

Discussion and Conclusions

It has been shown that suction of the boundary layer along the body just upstream of the leading edge of a wing-body junction has a significant effect on the horseshoe vortex. Specifically, 1) The size and significance of the large scale horseshoe vortex structure can be reduced by sucking off the upstream boundary layer which acts as the source of spanwise vorticity from which the horseshoe vortex is generated. This technique is far more successful than previous passive techniques. 2) A nondimensional volumetric flow rate of about 1.9 was required to almost totally suppress the large scale horseshoe vortex in the present experimental setup. 3) The streamwise edges of the rectangular suction hole used here acted as a streamwise vorticity source, thus making it impossible to reduce the circulation to zero.

It is probable that a small horseshoe vortex still exists, even in the higher suction flow rate experiments, because the no-slip condition requires the existence of a body boundary layer, however small. But this small boundary layer develops in a region where the flow is nearly stagnated, so the small scale vortex would be weaker than normally expected. A small and fairly weak vortex would have little effect on the flowfield, and it has thus been shown that body suction can virtually *eliminate* the wing-body junction vortex.

Further studies will need to be performed to address some of the concerns stemming from the above conclusions as well as other issues that are more applications-oriented in nature. The following are recommendations for future investigations:

1) More efficient suction geometries can be designed to reduce the suction hole edge vorticity production. The study performed by Goldsmith[8] on laminar flow control at a wing-body junction may give some guidance for future work.

2) The possibility of early separation off the wing when the approaching boundary layer is removed needs to be studied on a complete airfoil model at angle of attack; this problem was observed by Barber.[6]

3) The effectiveness of suction at off-design conditions needs to be evaluated. Here, suction flow rate is adjustable, and in that sense should be more adaptable than passive vortex suppression techniques.

In conclusion, it has been shown that the application of suction to the approaching boundary layer can reduce and even eliminate the large scale horseshoe vortex. This approach was shown to be capable of a more complete suppression of the horseshoe vortex than known passive techniques. Further research and development must be performed to determine the most efficient method of applying the suction, as well as to determine the effect of varying operating conditions.

Acknowledgments

Funds for this research were provided by Penn State's Applied Research Laboratory, for which the authors are grateful. The miniature five-hole probe was manufactured in-house by Harry E. Houtz, whose skill cannot be matched.

References

[1]Mehta, R. D., "Effect of Wing Nose Shape on the Flow in a Wing/Body Junction," *Aeronautical Journal*, Vol. 88, Dec. 1984, pp. 456–460.

[2]Kubendran, L. R., Bar-Sevar, A., and Harvey, W. D., "Flow Control in a Wing/Fuselage Type Juncture," AIAA Paper 88-0614, 26th Aerospace Sciences Meeting, Reno, NV, Jan. 1988.

[3]Sung, C. H., and Lin, C. W., "Numerical Investigation on the

Effect of Fairing on the Vortex Flows around Airfoil/Flat-Plate Junctures," AIAA Paper 88-0615, 26th Aerospace Sciences Meeting, Reno, NV, Jan. 1988.

[4]Devenport, W. J., Dewitz, M. B., Agarwal, N. K., Simpson, R. L., and Poddar, K., "Effects of a Fillet on the Flow Past a Wing Body Junction," AIAA Paper 89-0986, 2nd Shear-Flow Control Conf., Tempe, AZ, March, 1989.

[5]Maughmer, M., Hallman, D., Ruszkowski, R., Chappel, G., and Waitz, I., "Experimental Investigation of Wing/Fuselage Integration Geometries," *Journal of Aircraft*, Vol. 26, No. 8, 1989, pp. 705–711.

[6]Barber, T. J., "An Investigation of Strut-Wall Intersection Losses," *Journal of Aircraft*, Vol. 15, No. 10, 1968, pp. 676–681.

[7]McGinley, C. B., "Note on Vortex Control in Simulated Sail-Hull Interaction," *Journal of Ship Research*, Vol. 31, No. 2, 1987, pp. 136–138.

[8]Goldsmith, J., "Laminar Flow at the Juncture of Two Aeroplane Components," *Boundary Layer and Flow Control*, ed. by Lachmann, G. V., Pergamon Press, New York, Vol. 2, 1961, pp. 1000–1006.

[9]Press, W. H., Flannery, B. P., Teukolsky, S. A., and Vetterling, W. T., *Numerical Recipes, The Art of Scientific Computing*, Cambridge University Press, Cambridge, UK, Ch. 12, 1986.

[10]Philips, D. B., "An Experimental Investigation of the Effects of Body Surface Suction on the Wing-Body Junction Vortex," M.S. Thesis, The Pennsylvania State Univ., University Park, Dept. of Mechanical Engineering, PA, 1990.

[11]Dickinson, S. C., "Flow Visualization and Velocity Measurements in the Separated Region of an Appendage-Flat Plate Junction," David Taylor Naval Ship Research and Development Center, DTNSRDC Rept. 86/020, 1986.

[12]Devenport, W. J., and Simpson, R. L., "Time-Dependent Structure in Wing-Body Junction Flows," *Sixth Symposium on Turbulent Shear Flows*, Springer-Verlag, Berlin Heidelberg, 1989, pp. 231–248.

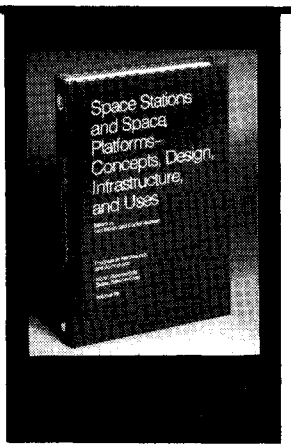

Space Stations and Space Platforms— Concepts, Design, Infrastructure, and Uses

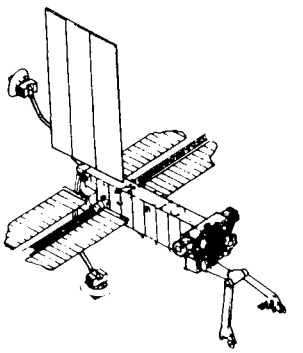

Ivan Bekey and Daniel Herman, editors

This book outlines the history of the quest for a permanent habitat in space; describes present thinking of the relationship between the Space Stations, space platforms, and the overall space program; and treats a number of resultant possibilities about the future of the space program. It covers design concepts as a means of stimulating innovative thinking about space stations and their utilization on the part of scientists, engineers, and students.

To Order, Write, Phone, or FAX:

AIAA

American Institute of Aeronautics and Astronautics
c/o Publications Customer Service,
9 Jay Gould Ct., P.O. Box 753
Waldorf, MD 20604 Phone: 301/645-5643 or 1-800/682-AIAA
Dept. 415 ■ FAX: 301/843-0159

1986 392 pp., illus. Hardback
ISBN 0-930403-01-0 Nonmembers $69.95
Order Number: V-99 AIAA Members $43.95

Sales Tax: CA residents, 8.25%; DC, 6%. For shipping and handling add $4.75 for 1–4 books (call for rates for higher quanties). Orders under $50.00 must be prepaid. Foreign orders must be prepaid. Please allow 4 weeks for delivery. Prices are subject to change without notice. Returns will be accepted within 15 days.

945